

# A physical map of the *Mamestra configurata* nucleopolyhedrovirus genome and sequence analysis of the polyhedrin gene

Sheping Li,<sup>1</sup> Martin Erlandson,<sup>2</sup> David Moody<sup>1</sup> and Cedric Gillott<sup>1</sup>

<sup>1</sup> Department of Biology, University of Saskatchewan, 112 Science Place, Saskatoon, SK, Canada S7N 5E2

<sup>2</sup> Agriculture and Agri-Food Canada, Saskatoon Research Centre, 107 Science Place, Saskatoon, SK, Canada S7N 0X2

The genome structure of a nucleopolyhedrovirus (NPV) isolated from the bertha armyworm, *Mamestra configurata* Walker (Lepidoptera: Noctuidae) (MacoNPV) was analysed with six restriction endonucleases (REN): *Bam*HI, *Eco*RI, *Hind*III, *Pst*I, *Sma*I and *Xho*I. More than 70 MacoNPV REN fragments were cloned into plasmids pUC18 and pBluescript SK(+). The physical map with 112 restriction sites for the above REN was constructed using double digests and Southern blot hybridization analysis of the MacoNPV DNA clones. The size of the DNA genome of the MacoNPV-90/2 isolate used for this study was estimated at 156 kbp based on REN fragment sizes. The position of the polyhedrin gene, which has by convention been used as the zero point of the REN maps of NPV, was determined by

hybridizing the *Autographa californica* multicapsid nucleopolyhedrovirus *Hind*III-V fragment clone, which contains most of the polyhedrin gene, with genomic blots of MacoNPV. The cloned MacoNPV fragments identified as containing the polyhedrin gene were sequenced and an ORF coding for a 246 amino acid polypeptide with 98.7% sequence identity with *Panolis flammea* nucleopolyhedrovirus (PafINPV) polyhedrin protein was identified. The putative polyhedrin gene sequence had 97.2% and 91.2% identity with the PafINPV and *Mamestra brassicae* multicapsid nucleopolyhedrovirus polyhedrin gene sequences, respectively, and also contained an upstream region identical to the highly conserved 12 bp consensus sequence TGTAAGT-AATTT typical of NPV very late genes.

## Introduction

The bertha armyworm, *Mamestra configurata* Walker (Lepidoptera: Noctuidae), is an important pest of cruciferous oilseed crops in western Canada. Although bertha armyworm populations are sporadic in their occurrence, during outbreak years larval densities exceed the economic threshold of 20 larvae/m<sup>2</sup> on an extensive acreage of canola (more than 600 000 ha in both 1994 and 1995). Seed yield losses in canola, ranging from 0.325 to 0.479 g per larva, are mainly caused by the last two (5th and 6th) larval instars feeding on the flower buds and developing seed pods (Bracken & Bucher, 1977). Currently, bertha armyworm populations are controlled by applications of chemical insecticides. Potential alternative control strategies, including various types of biological control, are under investigation. Pathogenic micro-organisms, including ento-

mophthoran fungi and baculoviruses, have been isolated from *M. configurata* populations across western Canada (Wylie & Bucher, 1977; Bucher & Turnock, 1983; Turnock, 1988; Erlandson, 1990). Mortality data from field populations of bertha armyworm larvae indicate that nucleopolyhedroviruses (NPVs) play only a minor role in regulating bertha armyworm at low host population densities, but may infect up to 30% of larval populations at high densities (Wylie & Bucher, 1977; Turnock, 1988). In certain cases, high levels of NPV infections occur where host larval populations were high in the preceding year and infection levels as high as 95% in late season populations of 4th- and 5th-instar larvae have been observed (Erlandson, 1990).

Several NPV isolates from *M. configurata* populations from single field sites were previously described as being multi-nucleocapsid types and designated as *M. configurata* multiple nucleopolyhedrovirus (MacoNPV) (Erlandson, 1990). These viruses were characterized by restriction endonuclease enzyme (REN) analysis of their DNA genomes and by SDS-PAGE analysis of virion structural polypeptides. In addition, bioassays indicated that the LD<sub>50</sub> values for two of the MacoNPV

**Author for correspondence:** Martin Erlandson.

Fax +1 306 956 7247. e-mail ErlandsonM@EM.AGR.CA

The GenBank accession number of the sequence reported in this paper is U59461.

isolates were approximately 20 occlusion bodies (OB) per neonate bertha armyworm larva, indicating the virus has potential as a biocontrol agent for bertha armyworm (Erlandson, 1990). Subsequently, additional MacoNPV strains were isolated from widely separate geographical populations of bertha armyworm (M. Erlandson, unpublished data). These isolates had small differences in their REN patterns but clearly were all closely related. Like the original MacoNPV isolates, all but one contained a heterogeneous mixture of genotypes as indicated by the presence of submolar REN bands. However, one isolate, MacoNPV-90/2, did not show submolar REN bands and was assumed to be a homogeneous isolate.

The present paper describes the cloning and physical mapping of the genome of the MacoNPV-90/2 isolate. The polyhedrin gene was also identified and sequenced. Analysis of the genome structure of MacoNPV and the genomic variation between geographical isolates of MacoNPV will be important for the definitive characterization of this virus and its potential as a biological control agent, for genetic engineering and gene mapping studies, and for comparisons with other viruses.

## Methods

**Insects, virus purification and viral DNA preparation.** Larvae from cultures of *M. configurata* were maintained on a semi-synthetic diet (Bucher & Bracken, 1976) at 21 °C, 60% relative humidity, and a 20:4 light/dark photoperiod. Stocks of MacoNPV were produced by infection of 4th-instar bertha armyworm larvae by contamination of the diet with  $1.4 \times 10^4$  OB/cm<sup>2</sup> of diet surface. Virus production and OB isolation, virion purification and viral DNA extraction essentially followed previously described methods (Erlandson, 1990). Briefly infected larvae were homogenized in sterile distilled water and MacoNPV OB purified by filtration and centrifugation following incubation in 0.5% SDS at 37 °C for 2 h. The OB were further purified by isopycnic centrifugation on sucrose gradients and the virions released from OB by incubation in alkaline OB dissolution buffer (0.1 M Na<sub>2</sub>CO<sub>3</sub>, 0.17 M NaCl, 0.001 M NaEDTA, pH 10.8) and purified by sucrose density centrifugation. Virus DNA was extracted from virion suspensions using the method of Smith & Summers (1978).

**REN analysis of viral DNA and cloning of viral DNA fragments.** Virus DNA was digested with *Bam*HI, *Eco*RI, *Hind*III, *Pst*I, *Sma*I and *Xho*I (GIBCO-BRL) at 37 °C for 2 to 3 h, then electrophoresed on 0.8%, 0.6% or 0.4% agarose gels at 50 V (1.5 V/cm) for 15 to 22 h to separate the fragments. Gels were stained with ethidium bromide and photographed on a Foto/PrepI (Fotodyne) transilluminator using Polaroid type 55 or type 57 positive/negative films. Negatives of gel films were scanned by densitometry and the sizes of viral DNA fragments were estimated using GelScan XL software (Pharmacia LKB).

Digested virus DNA was cloned into pUC18 or pBluescript SK(+) plasmid vectors and used to transform competent *E. coli* (DH5 $\alpha$ ) cells using standard techniques (Maniatis *et al.*, 1982). Specific viral REN fragment clones not generated by the shotgun cloning were excised from agarose gels and purified using GeneClean (Bio101) prior to cloning.

**In vitro labelling of DNA and Southern blot hybridization.** Viral genomic DNA and plasmids containing cloned virus DNA fragments were labelled with biotin *in vitro* using a BioNick nick translation kit (GIBCO-BRL) and used as probes in Southern blot hybridizations. Cloned viral fragment probes were made from miniprep

plasmid DNA. However, the 22 kbp *Hind*III-A viral genomic fragment, which we were unable to clone, was excised from an agarose gel and purified by centrifugation through siliconized glass wool and labelled with biotin (as above).

Viral DNA was digested with various REN, electrophoresed on 0.6% agarose gels, and the separated DNA fragments blotted onto PhotoGene nylon membranes (GIBCO-BRL). Membranes were prehybridized overnight at 42 °C in 50% formamide (25% formamide for low stringency hybridization), 6 $\times$  SSPE, 5 $\times$  Denhardt's solution, 1% (w/v) SDS, and 200  $\mu$ g/ml denatured salmon sperm DNA. DNA probes were hybridized to membranes overnight at 42 °C in 50% formamide (25% formamide for low stringency hybridization), 10% (w/v) dextran sulphate, 6 $\times$  SSPE, 5 $\times$  Denhardt's solution, 1% (w/v) SDS, and 200  $\mu$ g/ml denatured salmon sperm DNA. Membranes were washed in initial (2 $\times$  SSC, 0.1% SDS) and final (2 $\times$  SSC) wash buffers at room temperature for 5 min. For high stringency hybridizations, one intermediate wash was performed in 0.1 $\times$  SSC, 0.5% SDS at 50 °C for 30 min. For low stringency hybridizations, two intermediate washes were done in 6 $\times$  SSC, 0.1% SDS at 50 °C for 15 min each. DNA probes were detected on hybridized membranes using a PhotoGene Detection System (GIBCO-BRL) and X-AR or BioMax X-ray films (Kodak).

**Constructing the physical map of the viral genome.** The relative order of the restriction fragments on the viral genome was determined from the Southern blot hybridization data and double digests of cloned viral REN fragments. The zero point for the physical map was determined by hybridizing *Autographa californica* MNPV (AcMNPV) *Hind*III-V, containing the middle and 3' portion of the polyhedrin gene (Possee *et al.*, 1991), with Southern blots of MacoNPV genomic DNA. The AcMNPV *Hind*III-V fragment cloned in the plasmid polink26 was kindly provided by Tom Roberts (Veterinary Infectious Disease Organization, Saskatoon, Canada). The conventional practice of defining the REN fragment which contains the polyhedrin gene as the start point for physical maps of NPV (Vlak & Smith, 1982) was followed.

**DNA sequence analysis of REN fragments containing the polyhedrin gene.** Plasmids pMcH157, pMcEX5 and pMcHX2 containing cloned viral DNA were purified on Elutip mini-columns (Schleicher and Schuell) according to the manufacturer's instructions and sequenced by the dideoxynucleotide chain termination method at the DNA sequencing facility, Plant Biotechnology Institute, National Research Council of Canada, Saskatoon, Canada. Sequence data were generated from at least two different constructs for each plasmid, and the sequences were aligned and analysed using Lasergene software (DNASTAR).

## Results and Discussion

### Restriction endonuclease fragment analysis of MacoNPV isolate 90/2

Of the five MacoNPV strains isolated from different geographical areas of western Canada (M. Erlandson, unpublished data), the isolate MacoNPV-90/2 was selected for further analysis and physical mapping of the genome because the REN digestion pattern of this isolate had no submolar bands. This indicated that the isolate consisted of a single genotype, as opposed to a mixture of genotypes, at least as far as could be determined by REN digestion patterns. The DNA of MacoNPV isolate 90/2 was digested with *Eco*RI, *Hind*III, *Pst*I, *Bam*HI + *Sma*I, *Xho*I, *Bam*HI and *Sma*I with 26, 32, 24, 11, 19, 8 and 3 visible fragments detectable for each digest,

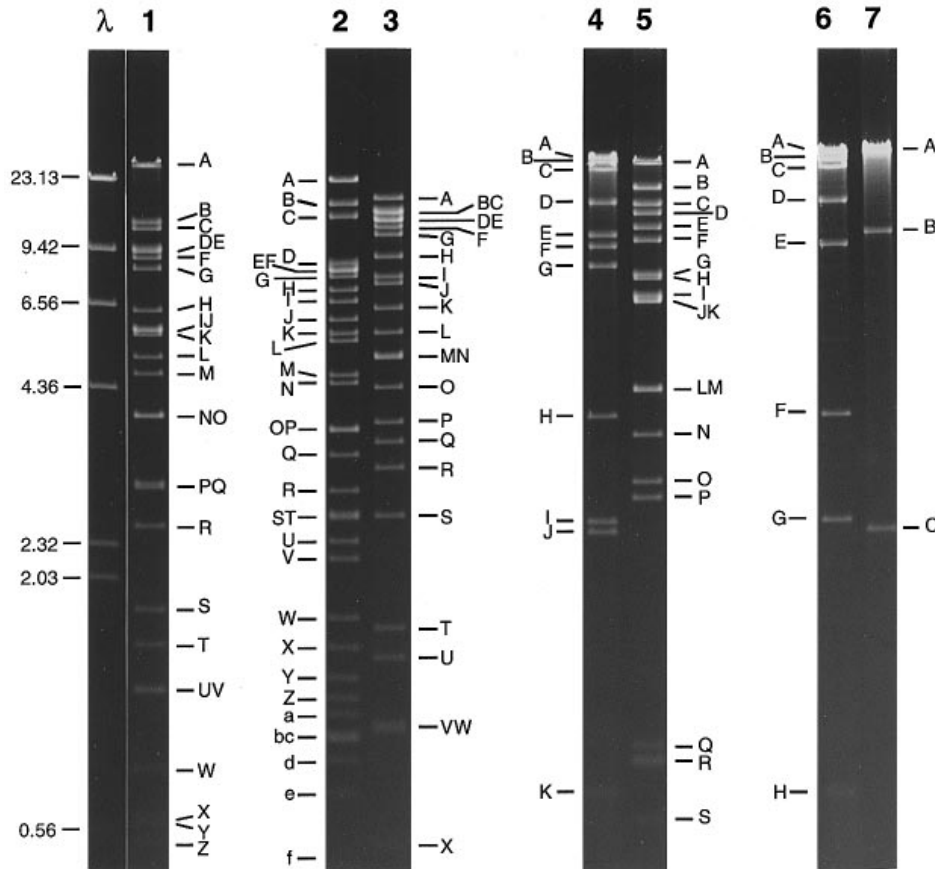


Fig. 1. REN fragment profiles of MacoNPV isolate 90/2 DNA digested with: *EcoRI* (lane 1), *HindIII* (lane 2), *PstI* (lane 3), *BamHI* + *SmaI* (lane 4), *XhoI* (lane 5), *BamHI* (lane 6) or *SmaI* (lane 7) and electrophoresed on a 0.6% agarose gel at 50 V for 17 h to separate the fragments. Lambda *HindIII* fragments ( $\lambda$ ) were used as size standards.

respectively (Fig. 1). The fragments were designated alphabetically starting with A for the largest fragment for each enzyme digest as proposed by Vlak & Smith (1982). Four sets of co-migrating fragments were detectable by stain intensity in the *HindIII* restriction pattern (*HindIII*-E&F, -O&P, -S&T and -b&c), five in the *EcoRI* pattern (*EcoRI*-D&E, -I&J, -N&O, -P&Q and -U&V), four in the *PstI* pattern (*PstI*-B&C, -D&E, -M&N and -V&W) and two in the *XhoI* pattern (*XhoI*-J&K and -L&M) (Fig. 1).

The size estimates for the REN fragments and the total genome size for MacoNPV-90/2 DNA are given in Table 1. These estimates are the means from 13 gels and were determined using densitometer scans comparing REN fragment mobilities with those of *HindIII*-digested  $\lambda$  DNA and/or GIBCO-BRL high molecular mass DNA standards. The mean size estimates for the complete MacoNPV-90/2 DNA genome ranged from 156.1 to 159.4 kbp, depending on the REN used, with a mean of 156.9 kbp (Table 1). This size estimate is considerably larger than the initial estimate of 144 kbp (Erlandson, 1990), due in part to the identification of additional small REN fragments not detected previously and a more precise estimate of the sizes of high molecular mass REN

fragments. The estimated size of the MacoNPV genome is also somewhat larger than certain of the better studied NPV including the AcMNPV variants (133 kbp) but similar to the size estimates for the *Mamestra brassicae* MNPV (MbMNPV) genome of 150 kbp (Possee & Kelly, 1988).

#### Recombinant plasmid library

All but one (*HindIII*-A) of the 32 *HindIII* fragments, 15 of the 26 *EcoRI* fragments, 10 of the 24 *PstI* fragments, 12 of the 19 *XhoI* fragments and one of the 11 *BamHI* + *SmaI* fragments (*BamHI* + *SmaI*-G) were cloned in recombinant plasmids (Table 1). The identity of the MacoNPV REN DNA fragments in all of the recombinant plasmids was confirmed by Southern blot hybridization to immobilized viral genomic DNA (data not shown). Recombinant clones representing all but 1.1% of the genome have been generated.

#### Hybridization results and the alignment of restriction endonuclease fragments

Data from Southern blot hybridizations using MacoNPV-90/2 recombinant clones as probes and REN-digested viral

**Table 1.** Size of restriction endonuclease fragments (kbp) of MacoNPV-90/2

Fragment	<i>Hind</i> III	<i>Eco</i> RI	<i>Pst</i> I	<i>Xho</i> I	<i>Bam</i> HI + <i>Sma</i> I
A	22·00	38·20	15·53	36·15	45·40
B	16·05*	12·20	13·25	18·35	35·40
C	13·66*	11·40	13·10	14·18	27·27
D	8·45*	9·55*	12·10*	12·78	14·20
E	8·11*	9·55	12·10*	10·88*	10·41
F	8·08*	9·02	11·20	9·86	9·30
G	7·73*	8·39	10·86	7·64*	8·14*
H	7·08*	6·42*	8·77	7·47	3·78
I	6·59*	5·84*	7·67*	6·66*	2·48
J	6·00*	5·84	7·34*	6·48*	2·38
K	5·61*	5·70*	6·32	6·48*	0·68
L	5·41*	5·10	5·59	4·20*	
M	4·57*	4·69*	4·98	4·20	
N	4·40*	3·92*	4·98	3·49*	
O	3·64*	3·92*	4·30	2·89*	
P	3·64*	2·96*	3·73	2·71*	
Q	3·29*	2·96*	3·45	0·84*	
R	2·85*	2·51	3·11*	0·76*	
S	2·58*	1·71	2·57*	0·55*	
T	2·58*	1·42	1·53*		
U	2·33*	1·11*	1·30*		
V	2·17*	1·11*	0·92*		
W	1·61*	0·76*	0·92*		
X	1·37*	0·59*	0·51*		
Y	1·17*	0·55*			
Z	1·06*	0·47*			
a	0·97*				
b	0·87*				
c	0·87*				
d	0·76*				
e	0·65*				
f	0·47*				
Total	156·62	155·89	156·13	156·57	159·44

\* Restriction endonuclease fragment has been cloned.

DNA immobilized on membranes were used to construct linear maps of MacoNPV-90/2 (Fig. 2). Data generated with probes of *Hind*III fragments were used to align the REN fragments. For example, the MacoNPV-90/2 *Hind*III-E (clone pMcH157) fragment hybridized to *Xho*I-J, -L and to a lesser degree to *Xho*I-N. The cloned MacoNPV-90/2 fragment *Hind*III-D also hybridized to *Xho*I-N and to *Xho*I-G. Thus, it was determined that *Hind*III-D was next to *Hind*III-E (pMcH157). In this fashion, the alignment of the REN fragments from various enzyme digests of MacoNPV was determined. For regions of the genome in which *Hind*III clones were not sufficient to define the order of REN fragments, cloned REN fragments from other enzyme digests were used as hybridization probes to determine REN alignments in detail. For example, the hybridization results using *Hind*III-U and *Hind*III-Y as probes showed that *Xho*I-E is at the left end of *Hind*III-G, and *Xho*I-R at the right end. However, this information was not sufficient

to determine the order of *Xho*I-M and *Xho*I-P. Because the *Pst*I-D clone (pMcP9) hybridized to *Xho*I-P and *Xho*I-E, but not *Xho*I-M, it could be deduced that *Xho*I-P is next to *Xho*I-E and is to the left of *Xho*I-M. In this fashion the detailed alignment of the REN DNA fragments of the MacoNPV-90/2 genome was determined. These data, as well as double digests of cloned virus DNA fragments (data not shown), were used to produce a physical map of the MacoNPV-90/2 which includes more than 110 restriction sites for the six REN investigated (Fig. 2).

The exact order of certain small restriction enzyme fragments could not be determined from the hybridization data. For example, both *Hind*III-a and *Hind*III-f hybridized to *Eco*RI-F, *Pst*I-F, *Xho*I-C, *Bam*HI-F and *Sma*I-A and their relative position could not be determined (data not shown). Those fragments for which the exact order could not be determined were positioned on the physical map using the convention of Vlak & Smith (1982) using double lettering (e.g. *Hind*III-a,f).

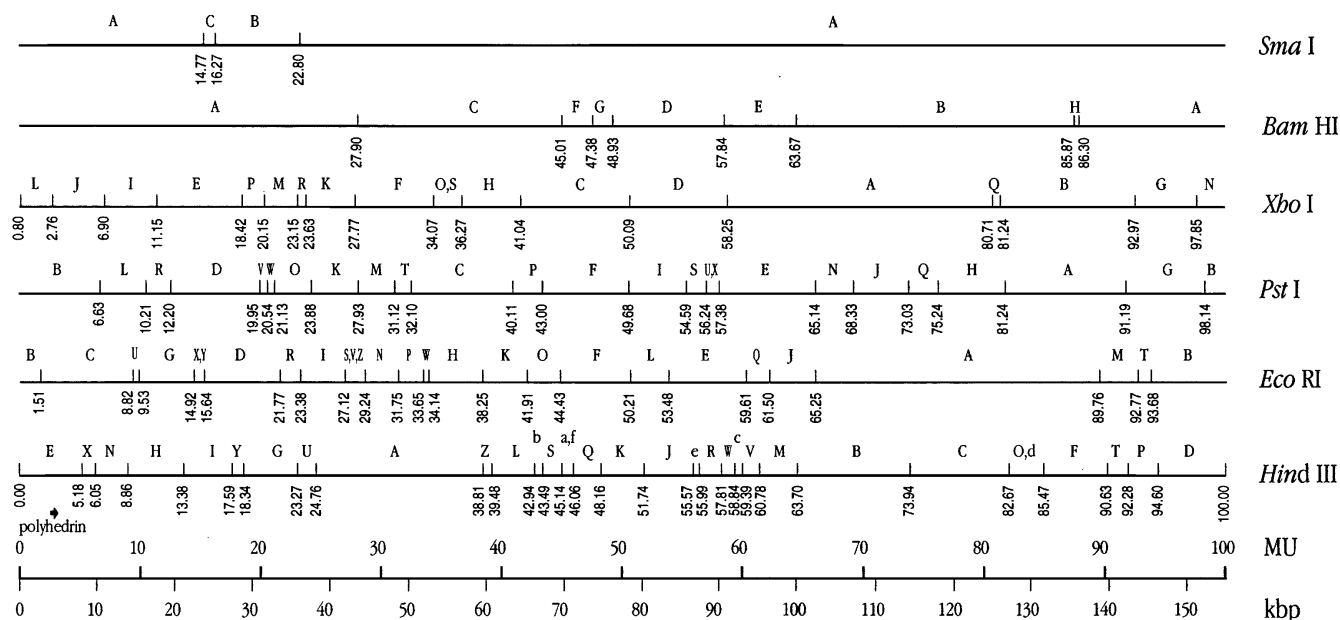


Fig. 2. Linearized physical map of MacoNPV-90/2 DNA for *Hind*III, *Eco*RI, *Xho*I, *Pst*I, *Bam*HI and *Sma*I. The total genome size of 156 kbp is indicated on a scale at the bottom below a map unit scale. The REN sites are indicated in map units (MU) from the zero point. The location of the polyhedrin gene is indicated with an arrow.

### Zero point of the physical map

Although Smith & Crook (1988) have suggested that the polyhedrin gene be used as the zero point of NPV REN map for more precision, we have used the convention of Vlak & Smith (1982) and designated the *Hind*III REN fragment containing the polyhedrin gene as the start site of a linearized physical map of MacoNPV. Southern blot hybridization using the pAc*Hind*III-V clone, which contains the 3' end of the AcMNPV polyhedrin gene, indicated that homologous sequences were located on the MacoNPV-90/2 *Hind*III-E (pMcH157), *Eco*RI-C, *Pst*I-B and *Xho*I-J and -L fragments (data not shown). The junction of *Hind*III fragments D and E (pMcH157) was assigned as the zero point of the linearized physical map based on the direction of transcription of the putative MacoNPV polyhedrin gene (see below) (Fig. 2).

### Cloning and sequencing of the polyhedrin gene

The MacoNPV *Hind*III-E fragment, which was identified as having sequences homologous to the AcMNPV polyhedrin gene and cloned in the recombinant plasmid pMcH157, was analysed by double digestion with *Hind*III plus either *Eco*RI or *Xho*I (Fig. 3a, lanes 1 and 2, respectively). Southern blot analysis using either pMcH157 (*Hind*III-E) (Fig. 3a, left panel) or pAc*Hind*III-V (right panel) clones as probes showed that AcMNPV polyhedrin sequences hybridized with the 5.35 kbp *Eco*RI-*Hind*III and 2.77 kbp *Xho*I-*Hind*III fragments at the right end of the clone (Fig. 3a, right panel; Fig. 3b). The 2.77 kbp *Xho*I-*Hind*III fragment, as well as the adjoining 2.58 kbp *Eco*RI-*Xho*I fragment, were subcloned into pBlue-

script SK(+) and designated pMcHX2.1 and pMcEX5.1, respectively. These clones were sequenced from the *Xho*I site using the T7 promoter and the sequencing strategy is summarized in Fig. 3(b). Custom primers designed to sequence across the *Xho*I site were used to confirm sequence on either side of the *Xho*I site. Analysis of the nucleotide sequence data from these MacoNPV DNA clones indicated the presence of a 738 nucleotide long ORF with a predicted coding capacity for a polypeptide of 246 amino acids (molecular mass 28 890 Da) (Fig. 4).

Comparison of the nucleotide sequence of the coding region of the ORF found in the region of the MacoNPV DNA, which is homologous to the AcMNPV polyhedrin gene, with others from sequence databases showed that it had 92% identity with the MbMNPV polyhedrin gene sequence (GenBank accession no. M20927) (Cameron & Possee, 1989) and 97% identity with the *Panolis flammea* nucleopolyhedrovirus (PafNPV) polyhedrin gene sequence (EMBL accession no. D00437) (Oakey *et al.*, 1989) (data not shown). This high degree of sequence identity with polyhedrin gene sequences from this presumably closely related NPV suggests that the ORF sequenced is the MacoNPV polyhedrin gene. The 100 bp of DNA sequence immediately upstream of the polyhedrin ATG start site is almost identical to those of PafNPV and MbMNPV differing at only four nucleotide positions (data not shown). This region spans a 12 bp consensus sequence (Fig. 4, bold and underlined) found upstream of all hyper-expressed very late NPV genes and includes the highly conserved TAAG element involved in transcription initiation (Rohrmann, 1986).

Similarly, when the predicted amino acid sequence deduced from the putative MacoNPV polyhedrin gene was compared

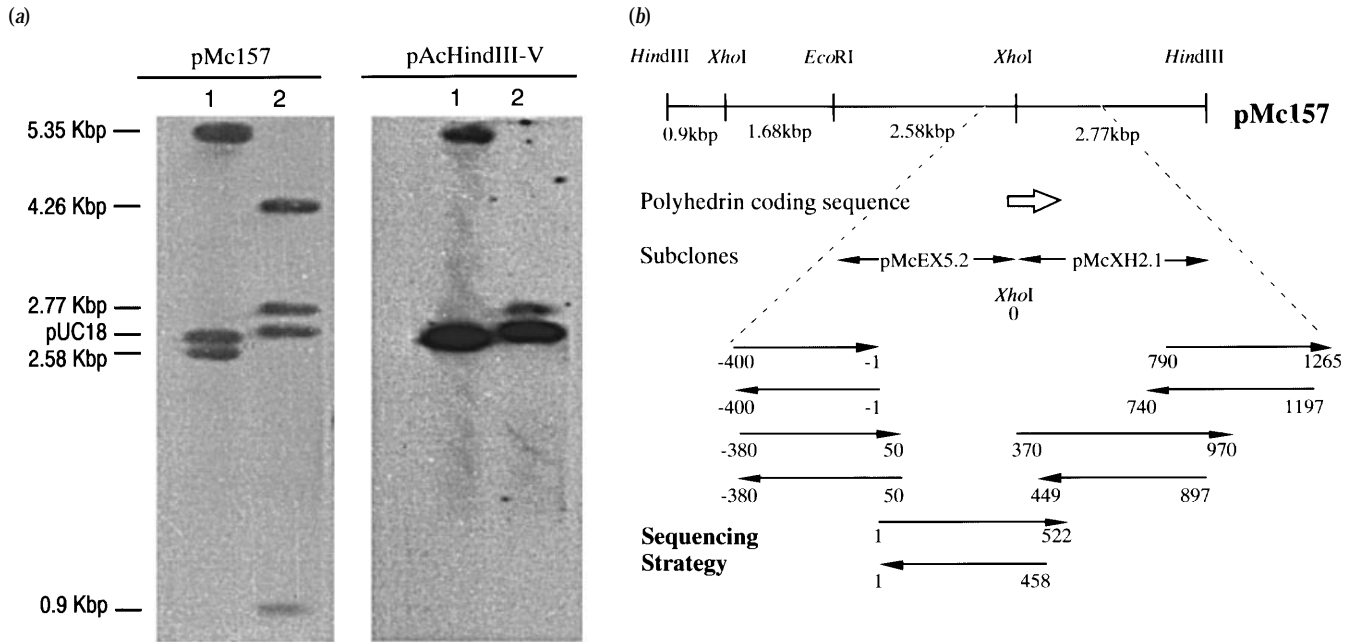


Fig. 3. Physical mapping, gene localization by hybridization and sequencing strategy of the polyhedrin gene region of MacoNPV. (a) Southern blot hybridization of MacoNPV *HindIII*-E (clone pMcH157) double digested with *HindIII* + *EcoRI* (lane 1) or *HindIII* + *XhoI* (lane 2) and probed with biotin-labelled DNA of either *HindIII*-E clone pMcH157 (left panel) or pAcMNPV *HindIII*-V fragment (AcMNPV polyhedrin gene) (right panel). (b) Physical map of MacoNPV *HindIII*-E fragment (clone pMcH157) and the strategy for subcloning and sequencing the polyhedrin gene. The arrows at the bottom of the figure indicate the size and direction of the DNA sequenced.

GCTTTACCACGTACATGATTGCACACAGTGTGATGGCGTCGGTTTCGTCGACGCGTATTTATATGTTTTTGGGAAATGTAAGTAATTTCTCCTTTCTGATAGAGATTGT 330  
 GAAAAATAAAATATAATGTATACCCGTTATAGTTACAACCCGTCGTTGGGACGTACCTACGTCCTACGACACAAGTACTACAAAAATCTAGGAGCAGTCATTAAGAACGC 440  
 M Y T R Y S Y N P S L G R T Y V Y D N K Y Y K N L G A V I K N A  
 CAACCGCAAGAAGCACTTTATCGAACATGAACCTCGAGGAGAAAACACTCGATCCCTAGACAGATTCTAGTGGCCGAGGACCCCTCTTTGGGACCGGGCAAAAACAAA 550  
 N R K K H F I E H E L E E K T L D P L D R F L V A E D P F L G P G K N Q  
 AGCTGACTCTCTTCAAAGAGATCAGAAATGTTAAGCCCGACACGATGAAGCTCGTGGTGAACCTGGAGCGGCAAGAGTTTCTCAGGGAACTTGGACCCGTTTTCATGGAA 660  
 K L T L F K E I R N V K P D T M K L V V N W S G K E F L R E T W T R F M E  
 GACAGCTTTCCCATCGTTAACGACCAAGAAGTCATGGATGTTTTCCCTCGTAATCAACATGCGTCCCACTAGACCCAACCCGTTGTTACAAAATTCCTGGCGCAGCATGCTCT 770  
 D S F P I V N D Q E V M D V F L V I N M R P T R P N R C Y K F L A Q H A L  
 GCGTTGCGATCCCGACTACGTGCCCCACGAAGTCATTGCGCATCGTTGAGCCATCATACTGGGCGAGCAACAACGAATACCGTGTGTCAGCTTGGCCAAGCGAGGCGGTGGCT 880  
 R C D P D Y V P H E V I R I V E P S Y V G S N N E Y R V S L A K R G G G  
 GCCCGTGATGAACCTGCACTCTGAGTACACCAACTCTTTGCAAGAGTTTCAACCGTGTGTCATCTGGGAGAACTTCTACAAGCCCATCGTGTACGTTGGTACCGATTGCG 990  
 C P V M N L H S E Y T N S F E E F I N R V I W E N F Y K P I V Y V G T D S  
 GCTGAGGAAGAAGAAATCCTCCTAGAGGTGCTCTGGTGTCAAAATCAAGGAGTTTGGCGCTGATGCACCTTTGTACAACGGACCGGCTTACTATAAATTCAAACACA 1100  
 A E E E E I L L E V A L V F K I K E F A P D A P L Y N G P A Y

Fig. 4. Nucleotide sequence of MacoNPV polyhedrin gene and flanking sequences. The polyhedrin gene coding sequence together with the deduced protein sequence are indicated. The polyhedrin transcription start site inferred by comparison with other polyhedrin genes is indicated as the 12 bp consensus sequence (underlined and bold). The polyhedrin translation start (ATG) and stop (TAA) codons are indicated (shaded and bold).

with the amino acid sequence of MbMNPV and PafNPV polyhedrins, it was shown to be nearly identical, being 97.6 and 98.7% similar to MbMNPV and PafNPV polyhedrins, respectively (Fig. 5). The deduced amino acid sequence of MacoNPV polyhedrin differs by only three amino acids from PafNPV polyhedrin. Although these amino acid changes do not occur in highly variable regions of polyhedrin (Zanotto *et*

*al.*, 1993), each of the changes is a very conservative substitution: phenylalanine for tyrosine at aa 54, aspartate for glutamate at aa 147 and alanine for serine at aa 226 (Fig. 5). The high degree of homology between the polyhedrin sequences of MacoNPV and PafNPV and MbMNPV indicates that MacoNPV would be classified in the Group II NPV as established by Zanotto *et al.* (1993). Group II NPV have

MacoNPV	( 1)	MYTRYSYNPSLGRTYVYDNKYKNLGAVIKNANRKKHFIEHELEEKTLDP
PafINPV	( 1)	.....
MbMNPV	( 1)	.....S.....R.Y.....
AcMNPV	( 1)	..PD...R.TI.....K.....A.....I.....A.....
MacoNPV	( 51)	LDRFLVAEDPFLGSPGKQKLTLFKEIRNVKPDTKLVVNWSGKEFLRETW
PafINPV	( 51)	...Y.....
MbMNPV	( 51)	...Y.....
AcMNPV	( 50)	..NY.....G.K.....Y.....
MacoNPV	( 101)	TRFMEDSFPVNDQEVMDVFLVINRPTRENRCKYFLAQHALRCDPDYVP
PafINPV	( 101)	.....E.....
MbMNPV	( 101)	.....F.....
AcMNPV	( 100)	..S.....V.....
MacoNPV	( 151)	HEVIRIVEPSPYVGSNNEYRVSLAKRGGGCPVNLHSEYTNSEFEFINRVI
PafINPV	( 151)	.....S.....
MbMNPV	( 151)	.....
AcMNPV	( 150)	.D.....W.....I.....K.....I.....Q.....D.....
MacoNPV	( 201)	WENFYKPIVYVGTDSAEIEEEIILEVALVFKIKEFAPDAPLYNGPAY
PafINPV	( 201)	.....S.....
MbMNPV	( 201)	.....S.....
AcMNPV	( 200)	.....I.....S.....V.....FT.....

Fig. 5. Comparison of the deduced polyhedrin protein sequence of MacoNPV with those of PafINPV (Oakey *et al.*, 1989), MbMNPV (Cameron & Possee, 1989), and AcMNPV (Hooft van Iddekinge *et al.*, 1983). Dots indicate identity of amino acid residues of PafINPV, MbMNPV and AcMNPV polyhedrin with that of the predicted amino acid sequence of MacoNPV polyhedrin.

polyhedrins with 246 amino acids instead of the 245 found in Group I. The MacoNPV, PafINPV and MbMNPV sequences are also identical for 5' sequences between the TAAG consensus sequence and the ATG start site of polyhedrin and are typical of Group II as opposed to Group I polyhedrin untranslated sequences (Zanotto *et al.*, 1993). Additional sequence information from the MacoNPV polyhedrin gene region indicated that there are two ORFs immediately downstream from the putative MacoNPV polyhedrin gene (data not shown). The first of these ORFs has a small region of homology to AcMNPV ORF 1629 and the second has significant homology to the AcMNPV PK1 gene. Each of these ORFs has an orientation with respect to coding strand and transcription direction similar to that of the AcMNPV genes. This points to a distribution of genes in this region of the MacoNPV genome similar to that which occurs in AcMNPV. It will be of interest to see how much similarity there is among these viruses as other gene sequences become available. The physical map of the MacoNPV-90/2 genome will serve as a framework for further studies of this viral genome, including additional MacoNPV gene mapping and cloning, investigation of the relationship between genomic structure and virulence differences among the geographic isolates of MacoNPV, and ultimately in genetic engineering of the virus to enhance its potential as a biological control agent.

We thank Dr M. Gruber and Dr R. Kutcher for their constructive review of this manuscript. We also wish to thank Mr R. Underwood for help in producing the figures. S.L. is a graduate student at the University of Saskatchewan, Saskatoon, Saskatchewan and was supported by a University of Saskatchewan post-graduate scholarship. This work was supported in part by a Canada-Saskatchewan Agricultural Green Plan Fund grant to M.E.

## References

- Bracken, G. K. & Bucher, G. E. (1977). An estimate of the relation between density of bertha armyworm (*Mamestra configurata*) and yield loss on rapeseed, based on artificial infestations. *Journal of Economic Entomology* **70**, 701–705.
- Bucher, G. E. & Bracken, G. K. (1976). The bertha armyworm, *Mamestra configurata* (Lepidoptera: Noctuidae). Artificial diet and rearing technique. *Canadian Entomologist* **108**, 1327–1338.
- Bucher, G. E. & Turnock, W. J. (1983). Dosage responses of the larval instars of the bertha armyworm, *Mamestra configurata* (Lepidoptera: Noctuidae), to a native nuclear polyhedrosis. *Canadian Entomologist* **115**, 341–349.
- Cameron, I. R. & Possee, R. D. (1989). Conservation of polyhedrin gene promoter function between *Autographa californica* and *Mamestra brassicae* nuclear polyhedrosis viruses. *Virus Research* **12**, 183–200.
- Erlanson, M. (1990). Biological and biochemical comparison of *Mamestra configurata* and *Mamestra brassicae* nuclear polyhedrosis virus isolates pathogenic for the bertha armyworm, *Mamestra configurata* (Lepidoptera: Noctuidae). *Journal of Invertebrate Pathology* **56**, 47–56.
- Hooft van Iddekinge, B. J. L., Smith, G. E. & Summers, M. D. (1983). Nucleotide sequence of the polyhedrin gene of *Autographa californica* nuclear polyhedrosis virus. *Virology* **131**, 561–565.
- Maniatis, T., Fritsch, E. F. & Sambrook, J. (1982). *Molecular Cloning: A Laboratory Manual*. Cold Spring Harbor, NY: Cold Spring Harbor Laboratory.
- Oakey, R., Cameron, I. R., Davis, B., Davis, E. & Possee, R. D. (1989). Analysis of transcription initiation in the *Panolis flammea* nuclear polyhedrosis virus polyhedrin gene. *Journal of General Virology* **70**, 769–775.
- Possee, R. D. & Kelly, D. C. (1988). Physical maps and comparative DNA hybridization of *Mamestra brassicae* and *Panolis flammea* nuclear polyhedrosis virus genomes. *Journal of General Virology* **69**, 1285–1298.
- Possee, R. D., Sun, T.-P., Howard, S. C., Ayres, M. D., Hill-Perkins, M. & Gearing, K. L. (1991). Nucleotide sequence of the *Autographa californica* nuclear polyhedrosis virus 9.4 kbp *EcoRI*-I and -R (polyhedrin gene) region. *Virology* **185**, 229–241.
- Rohmann, G. F. (1986). Polyhedrin structure. *Journal of General Virology* **67**, 1499–1513.
- Smith, G. E. & Summers, M. D. (1978). Analysis of baculovirus genomes with restriction endonucleases. *Virology* **89**, 517–528.
- Smith, I. R. L. & Crook, N. E. (1988). Physical maps of the genomes of four variants of *Artogeia rapae* granulosis virus. *Journal of General Virology* **69**, 1741–1747.
- Turnock, W. J. (1988). Density, parasitism, and disease incidence of larvae of the bertha armyworm, *Mamestra configurata* Walker (Lepidoptera: Noctuidae), in Manitoba, 1973–1986. *Canadian Entomologist* **120**, 401–413.
- Wylie, H. G. & Bucher, G. E. (1977). The bertha armyworm, *Mamestra configurata* Walker (Lepidoptera: Noctuidae). Mortality of immature stages on the rape crop, 1972–1975. *Canadian Entomologist* **109**, 823–837.
- Vlak, J. M. & Smith, G. E. (1982). Orientation of the genome of *Autographa californica* nuclear polyhedrosis virus: a proposal. *Journal of Virology* **41**, 1118–1121.
- Zanotto, P. M. de A., Kessing, B. D. & Maruniak, J. E. (1993). Phylogenetic interrelationships among baculoviruses: evolutionary rates and host associations. *Journal of Invertebrate Pathology* **62**, 147–164.

Received 18 June 1996; Accepted 4 September 1996